Spb4p, an essential putative RNA helicase, is required for a late step in the assembly of 60S ribosomal subunits in *Saccharomyces cerevisiae*

**JESÚS DE LA CRUZ,[1,]* DIETER KRESSLER,[1,]* MANUEL ROJO,[2] DAVID TOLLERVEY,[3]
and PATRICK LINDER[1]**

[1]Département de Biochimie Médicale, Centre Médical Universitaire, Université de Genève,
 CH-1211 Geneva, Switzerland
[2]Département de Biochimie, Sciences II, Université de Genève, CH-1211 Geneva, Switzerland
[3]Institute of Cell and Molecular Biology, University of Edinburgh, Edinburgh EH9 3JR, United Kingdom

ABSTRACT

Spb4p is a putative ATP-dependent RNA helicase that is required for synthesis of 60S ribosomal subunits. Polysome analyses of strains genetically depleted of Spb4p or carrying the cold-sensitive *spb4-1* mutation revealed an under-accumulation of 60S ribosomal subunits. Analysis of pre-rRNA processing by pulse-chase labeling, northern hybridization, and primer extension indicated that these strains exhibited a reduced synthesis of the 25S/5.8S rRNAs, due to inhibition of processing of the 27SB pre-rRNAs. At later times of depletion of Spb4p or following transfer of the *spb4-1* strain to more restrictive temperatures, the early pre-rRNA processing steps at sites A_0, A_1, and A_2 were also inhibited. Sucrose gradient fractionation showed that the accumulated 27SB pre-rRNAs are associated with a high-molecular-weight complex, most likely the 66S pre-ribosomal particle. An HA epitope-tagged Spb4p is localized to the nucleolus and the adjacent nucleoplasmic area. On sucrose gradients, HA-Spb4p was found almost exclusively in rapidly sedimenting complexes and showed a peak in the fractions containing the 66S pre-ribosomes. We propose that Spb4p is involved directly in a late and essential step during assembly of 60S ribosomal subunits, presumably by acting as an rRNA helicase.

Keywords: DEAD-box proteins; pre-rRNA processing; ribosome biogenesis; yeast

INTRODUCTION

The synthesis of eukaryotic ribosomes is a complex process that takes place largely, although not exclusively, in a specialized subnuclear compartment termed the nucleolus (Mélèse & Xue, 1995). There, the rDNA is transcribed as precursors (pre-rRNAs), which undergo processing, cleavage, and covalent modification. Concomitantly, these pre-rRNAs assemble with the ribosomal proteins (r-proteins) (reviewed in Woolford & Warner, 1991; Eichler & Craig, 1994; Tollervey & Kiss, 1997).

In *Saccharomyces cerevisiae*, three of four rRNAs (18S, 5.8S, and 25S) are produced as a single 35S pre-rRNA by RNA polymerase I, whereas the fourth rRNA (5S) is transcribed independently by RNA poly-

merase III (Woolford & Warner, 1991). In the 35S pre-rRNA, the mature rRNA sequences are separated by two internal transcribed spacers, ITS1 and ITS2, and flanked by two external transcribed spacers, 5′ ETS and 3′ ETS (see Fig. 1A). Maturation of this 35S pre-rRNA requires different *trans*-acting factors, including small nucleolar RNAs (snoRNAs), endonucleases, exonucleases, and rRNA modifying enzymes (van Nues et al., 1995; Venema & Tollervey, 1995; Tollervey & Kiss, 1997). Although the pre-rRNA processing pathway has been well-characterized (see Fig. 1B and its legend), the assembly process of the rRNAs and the r-proteins into mature ribosomal subunits is still poorly understood (Woolford & Warner, 1991). In the nucleolus, the pre-rRNAs associate with many of the r-proteins to form pre-ribosomal particles. The first pre-ribosome that can be detected is called 90S and contains the 35S pre-rRNA. From this particle, 66S and 43S pre-ribosomes are formed, containing the 27S and 20S pre-rRNAs, respectively (Trapman et al., 1975). The 66S particle remains in the nucleus for further process-
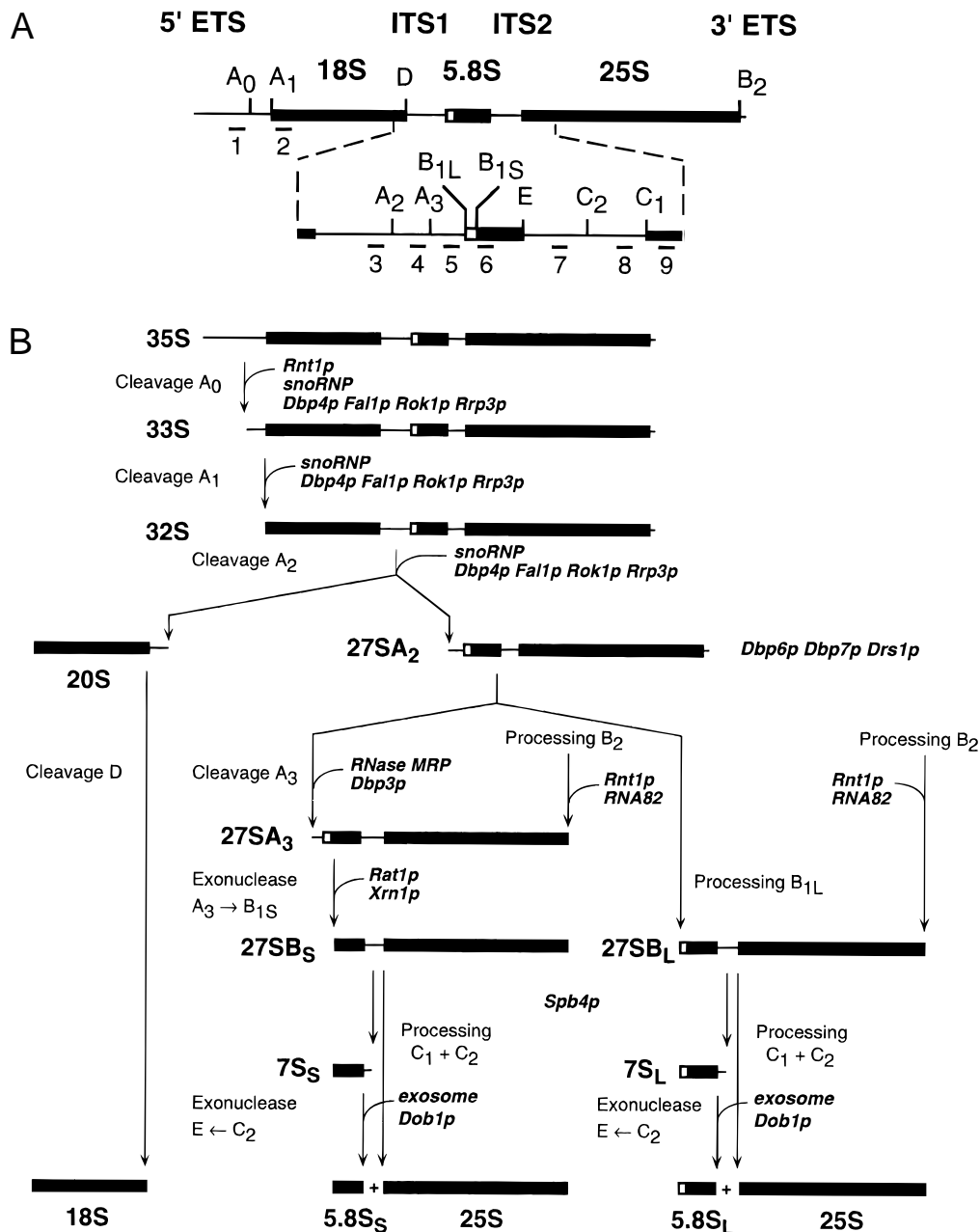
FIGURE 1. Pre-rRNA processing in *S. cerevisiae*. **A:** Structure of the 35S pre-rRNA and processing sites. This precursor contains the sequences for the mature 18S, 5.8S, and 25S rRNAs that are separated by the two internal transcribed spacers ITS1 and ITS2, and flanked by two external transcribed spacers, 5′ ETS and 3′ ETS. The location of various probes (numbered from 1 to 9) used in this study are indicated. Bars represent mature rRNA species and lines the transcribed spacers. **B:** Pre-rRNA processing pathway. The 35S pre-rRNA is cleaved at site A_0 by the endonuclease Rnt1p, generating the 33S pre-rRNA. This molecule is subsequently processed at sites A_1 and A_2, resulting in the separation of the pre-rRNAs destined for the small and large ribosomal subunits. The early pre-rRNA cleavages A_0 to A_2 are proposed to require a large snoRNP complex, which may be assisted by the putative ATP-dependent RNA helicases Dbp4p, Fal1p, Rok1p, and Rrp3p. The final maturation of the 20S precursor takes place in the cytoplasm, where endonucleolytic cleavage at site D yields the mature 18S rRNA. The $27SA_2$ precursor is processed by two alternative pathways that both lead to the formation of mature 5.8S and 25S rRNAs. In the major pathway, the $27SA_2$ precursor is cleaved at site A_3 by the RNase MRP complex. The putative ATP-dependent RNA helicase Dpb3p assists in this processing step. The $27SA_3$ precursor is exonucleolytically digested 5′ →3′ up to site B_{1S} to yield the $27SB_S$ precursor, a reaction requiring the exonucleases Xrn1p and Rat1p. A minor pathway processes the $27SA_2$ molecule at site B_{1L}, producing the $27SB_L$ pre-rRNA. While processing at site B_1 is completed, the 3′ end of mature 25S rRNA is generated by processing at site B_2. The subsequent ITS2 processing of both 27SB species appears to be identical. Cleavage at sites C_1 and C_2 releases the mature 25S rRNA and the 7S pre-rRNA. The latter undergoes exosome-dependent 3′ →5′ exonuclease digestion to the 3′ end of the mature 5.8S rRNA. It has been proposed that Dob1p/Mtr4p, a putative ATP-dependent RNA helicase, assists the exosome activity. The data presented in this study suggest that Spb4p is required for a late step in the assembly of 60S ribosomal subunits, a process that may also involve three other putative ATP-dependent RNA helicases Dbp6p, Dbp7p, and Drs1p.

ing, whereas the 43S pre-ribosome is exported rapidly to the cytoplasm, where the final maturation step in the synthesis of the 18S rRNA takes place (Udem & Warner, 1973; Trapman & Planta, 1976). A large number of r-proteins associate with the nucleolar pre-ribosomes at early steps in ribosome maturation, whereas another group assembles later (Kruiswijk et al., 1978). The available data are, however, far from being sufficient to establish any clear assembly pathway for the different r-proteins. In addition to r-proteins, the nucleolar pre-ribosomes have long been known to contain non-r-proteins (Trapman et al., 1975); the identity of these proteins has not been clearly established, but they presumably correspond to *trans*-acting factors required for pre-rRNA processing and modification or are involved in the assembly of the pre-rRNAs with the r-proteins.

Among the different *trans*-acting factors predicted to function enzymatically in ribosome biogenesis are the ATP-dependent RNA helicases. RNA helicases have been found in all organisms studied and are involved in many RNA metabolic processes, including translation initiation, pre-mRNA splicing, ribosome biogenesis, RNA degradation, and poly$(A)^+$ RNA export (Schmid & Linder, 1992; Fuller-Pace, 1994; Jacobs Anderson & Parker, 1996; Snay-Hodge et al., 1998; Staley & Guthrie, 1998; Tseng et al., 1998). For several of these proteins, an RNA-dependent ATPase activity has been found (for examples see Kim et al., 1992; O'Day et al., 1996b) and a small number of them have been shown to have an ATP-dependent RNA unwinding activity (for examples, see Rozen et al., 1990; Czaplinski et al., 1995; Schwer & Gross, 1998; Tseng et al., 1998; Wang et al., 1998). This class of proteins is therefore generally regarded as putative ATP-dependent RNA helicases. In yeast, the putative RNA helicases Dbp4p, Fal1p, Rok1p, and Rrp3p are required for 18S rRNA synthesis (O'Day et al., 1996a; Kressler et al., 1997; Liang et al., 1997; Venema et al., 1997), whereas Dbp3p, Dpb6p, Dbp7p, and Drs1p (Ripmaster et al., 1992; Weaver et al., 1997; Daugeron & Linder, 1998; Kressler et al., 1998) have been reported to be involved in the 25S/5.8S rRNA maturation and Dob1p/Mtr4p is required for correct 3′ end processing of the 5.8S rRNA (de la Cruz et al., 1998). In no case is the precise function of these enzymes understood, but, considering their presumed ATP-dependent RNA unwinding activities, RNA helicases are expected to be involved in structural rearrangements within the pre-ribosomal particles during pre-rRNA processing and assembly.

Spb4p is a putative RNA helicase that is essential for cell viability (Sachs & Davis, 1990). The cold-sensitive (cs) mutation *spb4-1* was isolated as one of seven different extragenic suppressor of the thermosensitive (ts) phenotype of a poly(A)-binding protein (Pab1p) mutant (*pab1-F364L*) (Sachs & Davis, 1989). Each of the *spb* (suppressor of poly(A)-binding protein) mutations, including *spb4-1*, led to decreased steady-state levels of free 60S ribosomal subunits (Sachs & Davis, 1989). In the case of *spb4-1*, this was due to reduced synthesis of the 25S rRNA, suggesting that Spb4p could be involved in the biogenesis of 60S ribosomal subunits (Sachs & Davis, 1990). However, the function of Spb4p has not been characterized further.

To learn more about the function of Spb4p, we have studied the subcellular localization of an HA-tagged Spb4p, and we have performed the detailed characterization of both a strain that expresses Spb4p conditionally and the *spb4-1* mutant. Our results indicate that Spb4 is a nucleolar protein required for normal processing of the 27SB precursors. We conclude that Spb4p is involved in the correct assembly of pre-ribosomal particles. In the absence of functional Spb4p, maturation of 60S ribosomal subunits is arrested at a late stage, leading to impaired production of mature 25S and 5.8S rRNAs from the 27SB pre-rRNAs, and finally to the depletion of mature 60S relative to 40S ribosomal subunits.

RESULTS

Conditional systems for the phenotypic analysis of Spb4p

The putative RNA helicase Spb4p is essential for cell viability (Sachs & Davis, 1990). Thus, two different conditional systems for phenotypic analysis were used to characterize its function. First, the *SPB4* ORF was placed under the control of an inducible *GAL* promoter, which allows expression of the gene in culture medium that contains galactose (YPGal) but is repressed in culture medium containing glucose (YPD). The resulting plasmid, pAS24-SPB4, expressed an N-terminally HA-tagged Spb4 fusion protein that fully complemented the *spb4* null strain (JDY8-1A) on YPGal and resulted in a severe slow-growth phenotype on YPD plates (Fig. 2A). In liquid YPGal medium, there was no difference in the growth rate between the *GAL::SPB4* (JDY8-1A pAS24-SPB4) and an isogenic wild-type *SPB4* strain (JDY8-1A YCplac111-SPB4). After transfer of the *GAL::SPB4* strain from liquid YPGal to YPD medium, the growth rate remained similar to that of the wild-type control strain for the first 12 h (doubling time 1.7 h), but it then decreased progressively to a doubling time of more than 10 h after 36 h in YPD (Fig. 2B). Western blot analysis (Fig. 2C) showed that the decrease in growth rate is preceded by depletion of HA-Spb4p.

In addition, we analyzed the *spb4-1* cs mutant (YAS168) (kindly provided by A. Sachs, University of California, Berkeley). This mutant showed a growth defect at 30 °C (doubling time 2.9 h for YAS168 versus 1.7 h for JDY8-1A YCplac111-SPB4 in YPD medium) that was enhanced at 18 °C (doubling time of more than 12 h for YAS168 versus 5.0 h for JDY8-1A
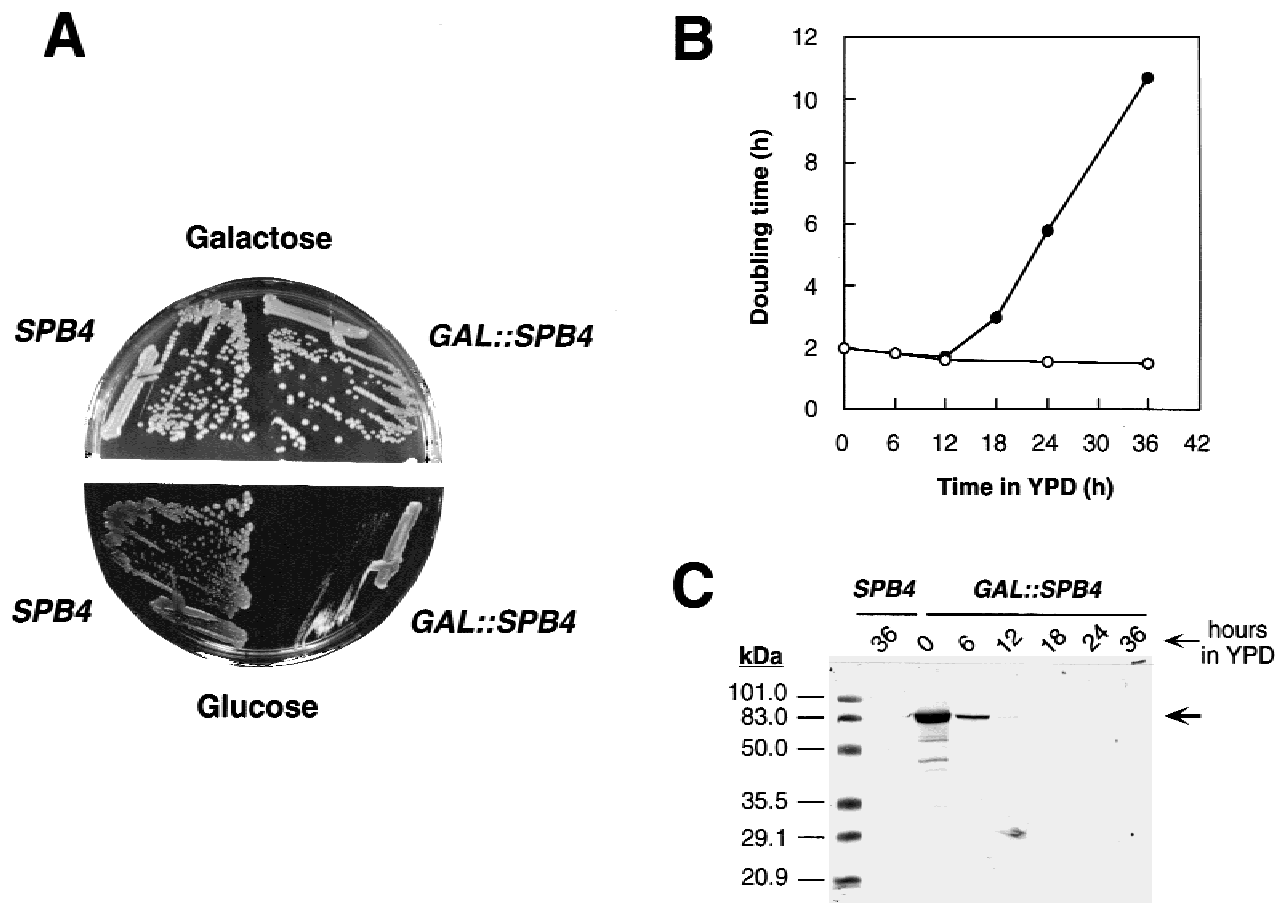
FIGURE 2. In vivo depletion of Spb4p. **A:** Growth comparison of JDY8-1A pAS24-SPB4 (*GAL::SPB4*) and its isogenic counterpart JDY8-1A YCplac111-SPB4 (*SPB4*). Cells were streaked on YPGal (Galactose) or YPD (Glucose) plates and incubated for 4 days at 30 °C. **B:** Growth curve of JDY8-1A pAS24-SPB4 (*GAL::SPB4*, closed circles) and JDY8-1A YCplac111-SPB4 (*SPB4*, open circles) at 30 °C after shifting logarithmic cultures from YPGal to YPD for up to 36 h. Data are represented as the doubling time at the different times in YPD. **C:** Depletion of Spb4p. The strains JDY8-1A YCplac111-SPB4 (*SPB4*) and JDY8-1A pAS24-SPB4 (*GAL::SPB4*) were grown in YPGal and shifted to YPD for up to 36 h. Cell extracts were prepared from samples harvested at the indicated times and assayed by western blotting. Equal amounts of total protein (around 70 μg) were loaded in each lane, as judged by Coomassie staining of gels or red Ponceau staining of the blots (data not shown). Prestained markers (Bio-Rad) were used as standards for molecular mass determination. Monoclonal mouse anti-HA 16B12 antibodies followed by alkaline phosphatase coupled goat anti-rabbit IgG were used to detect HA-Spb4p. The HA-Spb4p signal is indicated by an arrow. No signal was detected for untagged Spb4p (*SPB4*).

YCplac111-SPB4 in YPD medium). Transformation of YAS168 with a *CEN-SPB4* plasmid restored a wild-type growth rate, showing the *spb4-1* mutation to be recessive (data not shown).

The *GAL::SPB4* and *spb4-1* strains are deficient in 60S ribosomal subunits

To determine the effects of Spb4p depletion on ribosome metabolism, cell extracts were prepared from the *GAL::SPB4* and *SPB4* strains and subjected to sucrose gradient centrifugation. Polysome profiles and ratios of total ribosomal subunits were analyzed. As shown in Figure 3, depletion of Spb4p is accompanied by an overall decrease in polysomes, a deficit in free 60S ribosomal subunits, and the appearance of half-mer polysomes (Fig. 3A,B,C,D). Quantification of total

ribosomal subunits in low Mg^{2+} sucrose gradients indicated a deficit of total 60S ribosomal subunits relative to 40S subunits; an A_{254} 60S-to-40S ratio of around 2 was observed for *SPB4* in YPD or for *GAL::SPB4* grown in YPGal. This ratio decreased to around 1.2 after transfer of *GAL::SPB4* to YPD for 24 h (data not shown).

Polysome and total ribosomal subunit analyses were also performed with cell extracts prepared from *spb4-1* cells grown in YPD at permissive temperature (30 °C) or 12 h after transfer to the nonpermissive temperature (18 °C). The *spb4-1* mutation also led to a deficit of free 60S ribosomal subunits and the appearance of half-mer polysomes, the defect being more drastic after the shift to 18 °C (Fig. 3E,F). This defect can be fully reversed at either temperature by complementation of the *spb4-1* strain with a *CEN* plasmid harboring the wild-type *SPB4* gene (data not shown). When A_{254} 60S-
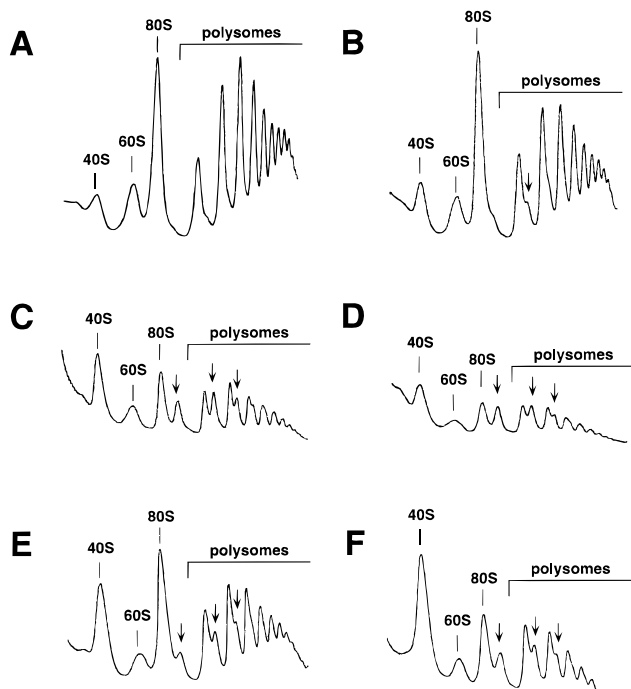
FIGURE 3. Depletion of Spb4p and the *spb4-1* mutation result in a deficit of free 60S ribosomal subunits and in the accumulation of half-mer polysomes. JDY8-1A pAS24-SPB4 was grown at 30 °C in YPGal and shifted to YPD for up to 24 h. Polysome analysis after (**A**) 6 h, (**B**) 12 h, (**C**) 18 h, and (**D**) 24 h. YAS168 was grown at (**E**) 30 °C or (**F**) shifted to 18 °C for 12 h. Cells were harvested at an OD$_{600}$ of 0.8, and cell extracts were resolved in 7–50% sucrose gradients. The A_{254} was measured continuously. Sedimentation is from left to right. The peaks of free 40S and 60S ribosomal subunits, 80S free couples/ monosomes, and polysomes are indicated. Half-mers are labeled by vertical arrows.

to-40S ratios were determined, the *spb4-1* mutant gave values of 1.5 (30 °C) and 1.3 (18 °C) compared to a value of 1.9 for the *spb4-1* strain complemented by a *CEN-SPB4* plasmid at either temperature.

Taken together, polysome and ribosomal subunit analyses indicated that the depletion of Spb4p and the *spb4-1* mutation led to similar reductions in the levels of 60S ribosomal subunits.

Formation of the mature 25S and 5.8S rRNAs is impaired upon Spb4p depletion

To further characterize the role of Spb4p in the metabolism of 60S ribosomal subunits, we first analyzed the effects of Spb4p depletion on synthesis and processing of pre-rRNA by [*methyl*-³H]methionine pulse-chase labeling experiments. For this purpose, JDY8-1A pAS24-SPB4 and JDY8-1A YCplac111-SPB4 were pre-grown in YPGal, then transferred to YPD for 13 h, and finally grown for 9 h (to an OD$_{600}$ of around 1) in synthetic medium lacking methionine (SD-Met). At this time point, the *GAL::SPB4* strain was doubling every 4.5 h compared with 2.5 h for the wild-type strain. The cells were

pulse-labeled for 1 min, then chased for 2, 5, and 15 min with an excess of cold methionine and total RNA was extracted and analyzed. In the wild-type *SPB4* strain, the 35S precursor was processed rapidly into 32S pre-rRNA and then into 27S and 20S species, the immediate precursors of the mature 25S and the 18S rRNA, respectively (Fig. 4A, lanes 1–4). In the Spb4p-depleted strain, we observed that processing of the 35S precursor was delayed (Fig. 4A, lane 5). Less 27SA species was formed, and the 27SB precursors per-
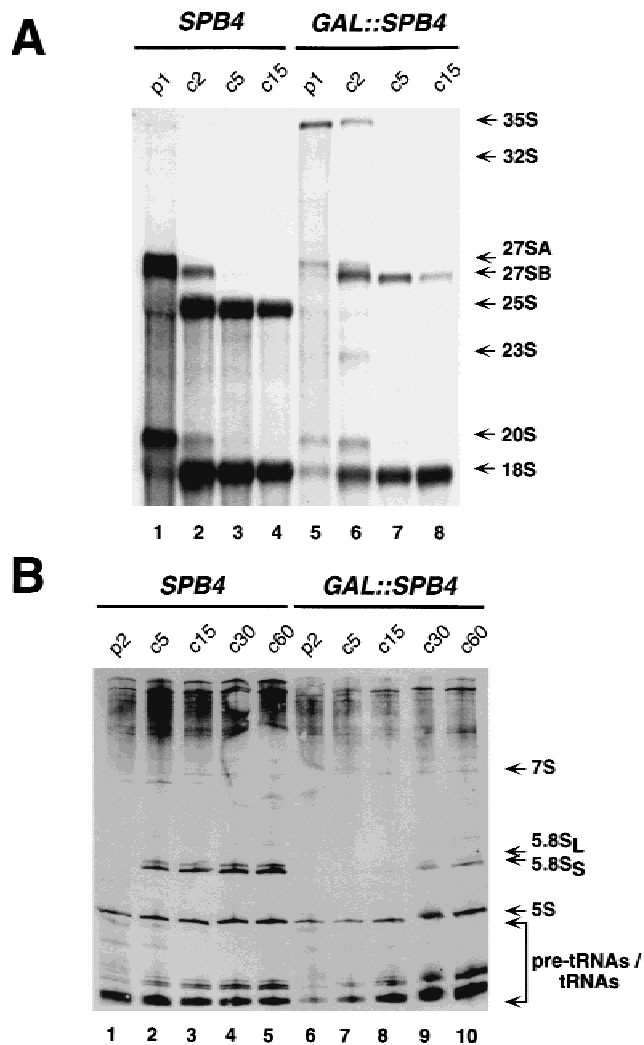
FIGURE 4. Depletion of Spb4p results in reduced synthesis of 25S and 5.8S rRNAs. **A:** Strains JDY8-1A YCplac111-SPB4 (*SPB4*) and JDY8-1A pAS24-SPB4 (*GAL::SPB4*) were grown at 30 °C in YPGal, shifted for 13 h to YPD, and then grown for 9 h in SD-Met. Cells were pulse-labeled with [*methyl*-³H]methionine for 1 min, and then chased with an excess of cold methionine for 2, 5, and 15 min. **B:** Strains JDY8-1A YCp50-SPB4 (*SPB4*) and JDY8-1A pAS24-SPB4 pRS416 (*GAL::SPB4*) were grown at 30 °C in SGal-Ura, and then shifted to SD-Ura for 22 h. Cells were pulse-labeled with [5,6-³H]uracil for 2 min, and then chased with an excess of cold uracil for 5, 15, 30, and 60 min. Total RNA was extracted and separated on 1.2% agarose–6% formaldehyde (**A**) or 7% polyacrylamide–50% urea gels (**B**), transferred to nylon membranes, and visualized by fluorography. Approximately 20,000 c.p.m. were loaded in each lane. The positions of the different pre-rRNAs and mature rRNAs and tRNAs are indicated.

sisted after the 15-min chase time point (Fig. 4A, lanes 5–8). As a consequence, almost no labeled mature 25S rRNA was detected (Fig. 4A, lane 8). The processing pathway leading to the formation of 18S rRNA was also mildly impaired, as revealed by the lower levels of mature 18S rRNA (Fig. 4A, lanes 7, 8) and its 20S precursor (Fig. 4A, lanes 5, 6). An aberrant 23S species was also detected (Fig. 4A, lane 6). However, the kinetics of processing of the 20S precursor to the mature 18S rRNA was not affected.

To exclude a defect in rRNA methylation and to monitor the synthesis of low-molecular-weight RNAs, cells were also pulse-labeled with $[5,6\ ^3H]$uracil. Strains JDY8-1A pAS24-SPB4 pRS416 and JDY8-1A YCp50-SPB4 were pre-grown in SGal-Ura and then transferred to SD-Ura for 22 h (to an OD_{600} of around 1). At this time point, the *GAL::SPB4* strain was doubling every 3.6 h compared with 2 h for the isogenic *SPB4* strain. The cells were pulse-labeled for 2 min and then chased for 5, 15, 30, and 60 min with an excess of cold uracil. Analysis of high-molecular-weight RNAs gave results comparable to those shown in Figure 4A (data not shown). Analysis of low-molecular-weight RNAs showed that the synthesis of mature 5.8S rRNAs was both substantially delayed and strongly reduced following Spb4p depletion. In contrast, synthesis of the 5S rRNA and tRNAs was comparable both in kinetics and efficiency in wild-type and Spb4p-depleted cells (Fig. 4B).

These results indicated that the deficit in 60S ribosomal subunits following Spb4p depletion was due to the inhibition of processing of the 27SB precursors to mature 25S and 5.8S rRNAs. A defect in earlier processing reactions on the pathway of 18S rRNA synthesis was also observed.

## Pre-rRNA processing is inhibited by depletion of Spb4p

To define the pre-rRNA processing steps that are affected in the conditional *spb4* strains, steady-state levels of mature rRNAs and pre-rRNA intermediates were assessed by northern and primer extension analyses. Total RNA was isolated from the *GAL::SPB4* and an isogenic *SPB4* strain at various time points after transfer from YPGal to YPD and analyzed by northern hybridization. As shown in Figure 5A, depletion of Spb4p resulted in a slight decrease in 18S rRNA and in a more drastic decrease in 25S rRNA. Oligonucleotides, hybridizing to sites in the 35S pre-rRNA transcript (see Fig. 1A), were used to identify the processing intermediates. Slight differences in the levels of the pre-rRNAs observed between the 0 h and 36 h time points for the wild-type strain are due to the effects of a nutritional up-shift from galactose to glucose medium; comparable increases in the levels of several pre-rRNA species are seen in the *GAL::SPB4* strain at early

times (6 h and 12 h) after transfer to glucose medium. Consistent with the pulse-chase labeling results, the *GAL::SPB4* strain accumulated the 35S pre-rRNA; clear accumulation was observed 12 h after transfer to glucose and increased with time (Fig. 5B,C,D,E,F, lanes 5–8). The 27SB pre-rRNA was strongly accumulated at 12 h and at later time points (shown for probe 8 in Fig. 5F; probe 7 gave identical results, data not shown). The aberrant 23S RNA also appeared, commencing 18 h after transfer to glucose medium (Fig. 5B,C,D, lanes 6–8). This species extends from the 5′ ETS to site A_3, as shown by its hybridization with probes 1 and 4 (Fig. 5B,D), but not with oligonucleotide 5 (Fig. 5E). The levels of the 20S (Fig. 5C, lanes 7, 8) and $27SA_2$ pre-rRNAs (Fig. 5D,E, lanes 7, 8) are reduced in the Sbp4p-depleted strain, commencing 18 h after transfer to glucose medium. However, 12 h after transfer to glucose, 27SA pre-rRNAs accumulated (Fig. 5D,E, lane 5). Analysis of low-molecular-weight rRNA species revealed a slight decrease in the steady-state levels of the 7S pre-rRNA and 5.8S rRNAs, but no alteration in the levels of 5S rRNA in the Spb4p-depleted strain (data not shown). The ratio of $5.8S_S$ and $5.8S_L$ rRNAs was not affected by Spb4p depletion (data not shown).

We conclude that, approximately 12 h after transfer of the *GAL::SPB4* strain to glucose medium, pre-rRNA processing was inhibited at sites C_1 and C_2. Approximately 18 h after transfer to glucose, cleavage started to be inhibited at the early processing sites A_0, A_1, and A_2, with increasing inhibition at later time points.

Because northern hybridization does not distinguish between the $27SA_2$ and $27SA_3$, and between the $27SB_L$ and $27SB_S$ precursors, we assessed the levels of these species by primer extension analyses, using oligonucleotides 5 and 8 as primers (see Fig. 1A). The primer extension stops at sites B_{1L} and B_{1S} increased at 12 h and later times after transfer to glucose medium (Fig. 6, upper panel), indicating that both $27SB_L$ and $27SB_S$ were accumulated upon depletion of Sbp4p. The level of the primer extension stop at site A_2, the 5′ end of the $27SA_2$ pre-rRNA, increased 12 h after transfer to glucose medium (Fig. 6, upper panel, lane 5), but was reduced strongly at later time points (Fig. 6, upper panel, lanes 7, 8), fully consistent with the results obtained by northern hybridization. A similar observation was made for site A_3, the 5′ end of the $27SA_3$ pre-rRNA (Fig. 6, bottom panel, lanes 5, 7, and 8). The level of the $27SA_3$ pre-rRNA was, however, reduced to a lesser extent than $27SA_2$. Finally, primer extension analysis also showed that processing at all these sites was accurate at the nucleotide level during the time course of Spb4p depletion.

Similar hybridization and primer extension analyses were performed on total RNA extracted from the *spb4-1* mutant and from a *SPB4* control strain grown at 30 °C or shifted for 12 h to 18 °C. These analyses revealed that the *spb4-1* mutation led at 30 °C and at 18 °C to
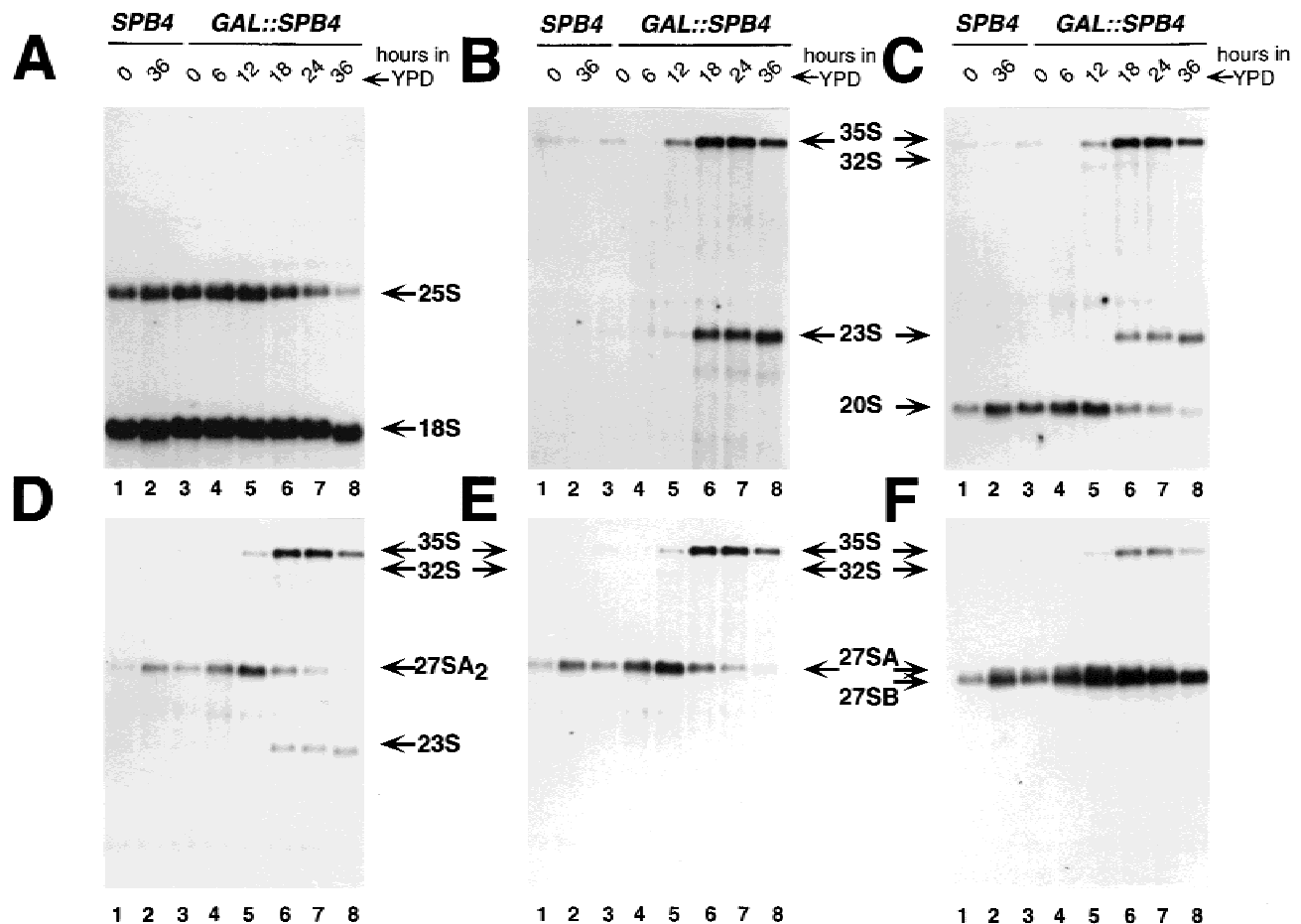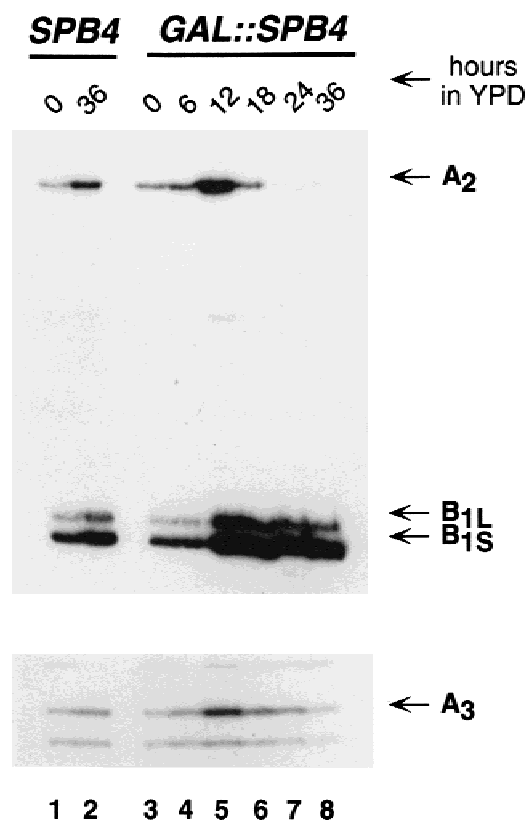
FIGURE 5. Depletion of Spb4p affects the steady-state levels of pre-rRNA and mature rRNA species. The strains JDY8-1A YCplac111-SPB4 (*SPB4*) and JDY8-1A pAS24-SPB4 (*GAL::SPB4*) were grown in YPGal and shifted for up to 36 h to YPD. Cells were harvested at the indicated times and total RNA was extracted. Equal amounts of total RNA (5 μg) were resolved on a 1.2% agarose–6% formaldehyde gel and transferred to a nylon membrane for northern hybridization. The same filter was consecutively hybridized with all the different probes used. **A:** Hybridization with probe 2 and 9 (see Fig. 1A for location of the probes), base pairing to sequences within the mature 18S and 25S rRNAs, respectively. **B:** Probe 1 in the 5′ ETS. **C:** Probe 3 in ITS1, between the sites D and A_2. **D:** Probe 4 in ITS1, between the sites A_2 and A_3. **E:** Probe 5, 3′ to site A_3. **F:** Probe 8 in ITS2, between the sites C_2 and C_1. Positions of the different pre-rRNAs and mature rRNAs are indicated by arrows.

effects similar to those observed after 12 h and 24 h of Spb4p depletion, respectively. At 30 °C, there was an accumulation of the 27SA and 27SB pre-rRNA species in *spb4-1* cells, but no clear alteration in other precursors. After a shift to 18 °C for 12 h, the *spb4-1* strain showed an accumulation of the 35S and 23S pre-rRNAs and strong accumulation of both 27SB pre-rRNAs. The levels of the 20S and 27SA precursors were reduced markedly, whereas levels of the 7S pre-rRNA and the 5.8S and 25S rRNAs were only reduced mildly (data not shown).

Together, these data demonstrated that depletion of Spb4p and the *sbp4-1* mutation led to similar pre-rRNA processing defects. At early times of depletion or with the *sbp4-1* strain at 30 °C, processing of the 27SB pre-rRNAs at C_1 and C_2 was inhibited, leading to depletion of the mature 25S and 5.8S rRNAs. At later times of depletion or with the *sbp4-1* strain at 18 °C, pre-rRNA cleavages at sites A_0, A_1, and A_2 were also inhibited.

The 27SB pre-rRNAs accumulate in pre-ribosomal particles

In wild-type cells, the 27SB pre-rRNAs are present in 66S pre-ribosomal particles (Trapman et al., 1975). We therefore analyzed whether these particles assemble in the absence of functional Spb4p. Cells from *spb4-1* and *SPB4* strains were grown in YPD at 30 °C and shifted for 12 h to 18 °C. Cell extracts were fractionated on sucrose gradients containing a low concentration of Mg^{2+}, in which ribosomes and polysomes dissociate into free ribosomal subunits (Foiani et al., 1991). RNA was recovered from each fraction and pre-rRNAs and mature rRNAs were analyzed by northern hybridization. In both wild-type and *spb4-1* cell extracts, the mature 25S and 18S rRNAs were found at positions on the gradients corresponding to the 60S and 40S peaks, respectively (Fig. 7A,B, fractions 5 and 7–8, respectively). The 20S pre-rRNA co-fractionated with the ma-

FIGURE 6. Depletion of Spb4p leads to higher steady-state levels of the 27SB precursors. The strains JDY8-1A YCplac111-SPB4 (*SPB4*) and JDY8-1A pAS24-SPB4 (*GAL::SPB4*) were grown in YPGal and shifted for up to 36 h to YPD. Cells were harvested at the indicated times and total RNA was extracted. Primer extension with oligonucleotide 8 within ITS2 reveals the processing sites B_{1S}, B_{1L}, and A_2 (upper panel). The lower panel corresponds to a primer extension with oligonucleotide 5, priming 3′ to site A_3 and reveals the processing at this site. Arrows indicate the positions of the primer extension stops corresponding to the different pre-rRNA species analyzed.

ture 18S rRNA in both wild-type and *spb4-1* cell extracts (Fig. 7A,B, fraction 5). In wild-type extracts, the majority of 27SA and 27SB pre-rRNAs was found in fractions of higher sedimentation coefficient than 60S (Fig. 7A, fraction 8 and data not shown). In *spb4-1* extracts, 27SA pre-rRNAs were almost undetected (data not shown), but a strong hybridization signal was obtained for the 27SB pre-rRNAs (Fig. 7B, fraction 9). In both strains, the 27SB pre-rRNAs sedimented below the mature 25S rRNA. Interestingly, the 23S pre-rRNA detected in the *spb4-1* cells also sedimented below the major 60S peak (Fig. 7B, fractions 9–10), despite having an RNA component that is shorter than the 25S rRNA. Finally, a weak signal corresponding to the 35S pre-rRNA was detected in a fraction with an even higher sedimentation coefficient than that containing the 27SB pre-rRNAs (fractions 11–12 for both wild-type and *spb4-1* cell extracts; data not shown).

Together, these results indicated that in both wild-type and *spb4-1* cells, the 35S, 27S, and 20S pre-rRNAs

were present in the form of high-molecular-weight complexes, most likely corresponding to the previously identified 90S, 66S, and 43S pre-ribosomal particles, respectively (Trapman et al., 1975). In the *spb4-1* mutant, the 27SB pre-rRNAs accumulated in a pre-ribosomal particle, which did not clearly differ in sucrose gradient mobility from the wild-type particle. It has been suggested that the 90S pre-ribosomes are split into the 66S and 43S pre-ribosomal particles after cleavage of the 35S pre-rRNA at site A_2 (van Nues et al., 1995). No co-sedimentation of the 20S and 27SA/B pre-rRNAs was observed, indicating that the 66S and 43S pre-ribosomal particles dissociate rapidly on cleavage of the 35S pre-rRNA. Our results also showed that the aberrant 23S rRNA is found in a particle of higher sedimentation coefficient than 43S, but lower than 90S, presumably indicating that this particle remains associated with processing and/or assembly factors that dissociate from the 20S pre-rRNA following cleavage.

Spb4p is required for processing of the 27SB pre-rRNAs within the 66S pre-ribosomal particles. We therefore determined whether Spb4p is also a component of these particles. For this purpose, Spb4p was HA-tagged at its N-terminus and expressed from its authentic promoter on a *CEN* plasmid (YCplac111-HA-SPB4). This plasmid complemented the *spb4* null allele to the wild-type extent at all temperatures tested (18, 30, and 37 °C), indicating that the HA-Spb4 fusion protein was fully functional. Western-blot analysis with a mouse monoclonal anti-HA antibody detected a single protein with a molecular mass of 85 kDa in a total cell extract from the strain expressing the HA-tagged Spb4p (JDY8-1A YCplac111-HA-SPB4), but not from the *SPB4* strain (JDY8-1A YCplac111-SPB4) (data not shown). Sucrose gradient fractionation was performed with cell extracts from the strain expressing HA-Sbp4p and fractions were analyzed by western blot analysis. Ssm1p, which is a 60S r-protein (Petitjean et al., 1995), was used as a marker for the sedimentation of 60S ribosomal subunits. The small nucleolar ribonucleoparticle (snoRNP) protein Nop1, which is expected to be associated with the pre-ribosomal particles, was also used as a control. As shown in Figure 8, Ssm1p was found exclusively associated with fractions corresponding to the mature 60S ribosomal subunits and the putative 66S pre-ribosomal particle (Fig. 8, fractions 6–8). Little HA-Spb4p or Nop1p sedimented at the positions expected for the free proteins (Fig. 8, fractions 1 and 2), although overexposure of the blots indicated the existence of very minor pools of both proteins (data not shown). A peak of HA-Spb4p was found in fractions corresponding to the 66S pre-ribosomal particle (Fig. 8, fractions 7 and 8); these fractions also contained the peak of the 27SB pre-rRNAs (data not shown). Lower amounts of HA-Spb4p were detected lower on the gradient, in fractions that contain the 35S pre-rRNA, presumably corresponding to the 90S pre-
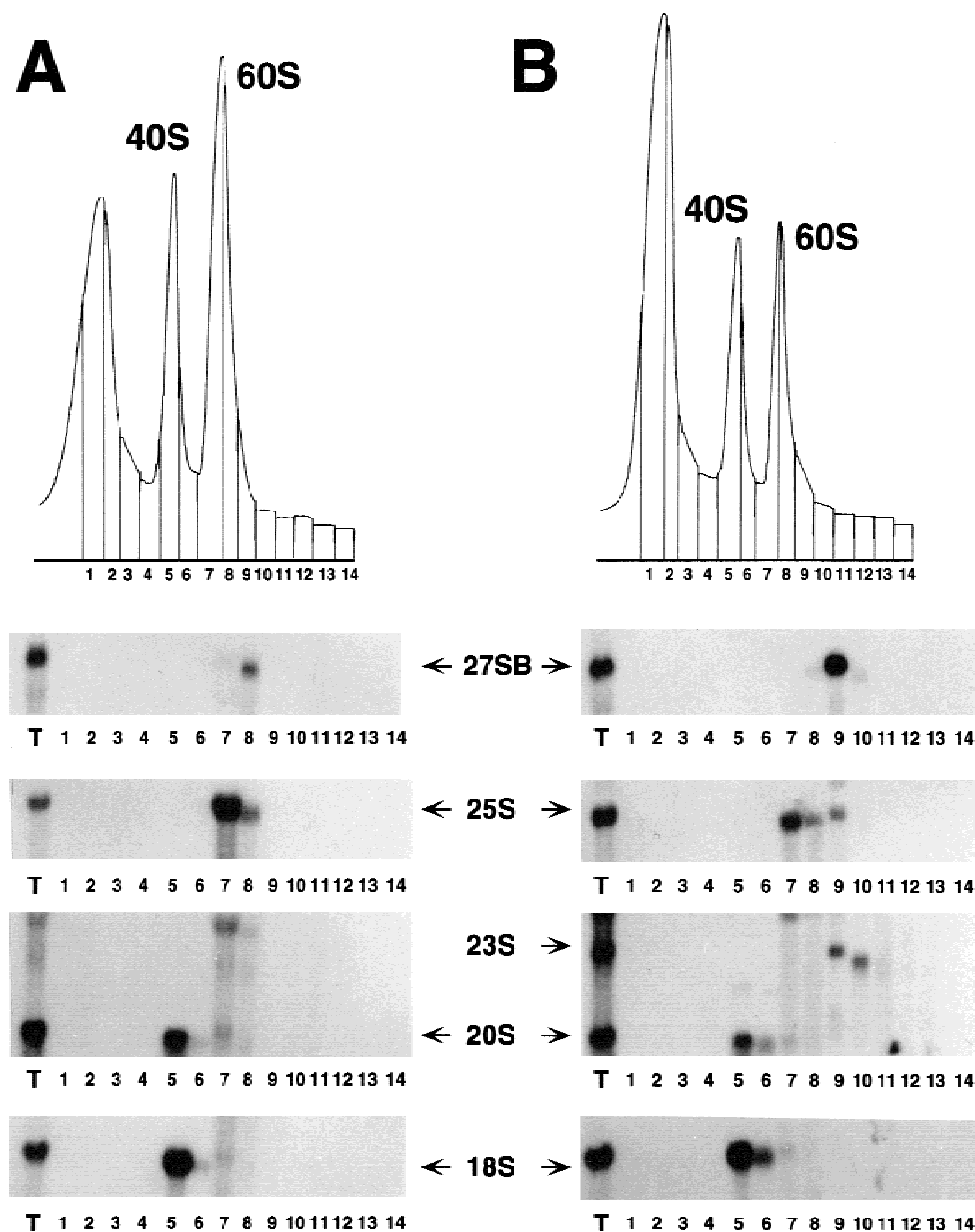
FIGURE 7. The 27SB pre-rRNAs accumulate in 66S pre-ribosomal particles. Wild-type (YAS168 YCplac111-SPB4) (**A**) and *spb4-1* (YAS168) cells (**B**) were grown at 30 °C in YPD and shifted to 18 °C for 12 h. Cells were harvested at an OD_{600} of 0.8. Cell extracts were resolved in 7–50% sucrose gradients containing a low concentration of Mg^{2+} to dissociate ribosomes into subunits. The A_{254} was measured continuously. Sedimentation is from left to right. The peaks of free material and total 40S and 60S ribosomal subunits are indicated. Fractions were collected and RNA was extracted from each fraction. T stands for total extract and numbers indicate the fraction numbers. Equal volumes were resolved on a 1.2% agarose–6% form-aldehyde gel and transferred to a nylon membrane for northern hybridization. The same filters were hybridized consecutively with different probes to detect the different pre-rRNAs and mature rRNAs indicated by the arrows.

ribosomes (Fig. 8, fractions 9–11). Both HA-Spb4p and Nop1p were also found in fractions above the 40S subunits. In the case of Nop1p, this presumably represented the population of snoRNPs that was not engaged with the 35S pre-rRNA at the moment of cell lysis.

We conclude that HA-Spb4p is almost entirely present in relatively large complexes in cell lysates. The sedimentation of these overlapped the positions of the 60S ribosomal subunits and 66S pre-ribosomes, and is similar to that of Nop1p. These data are consistent with the
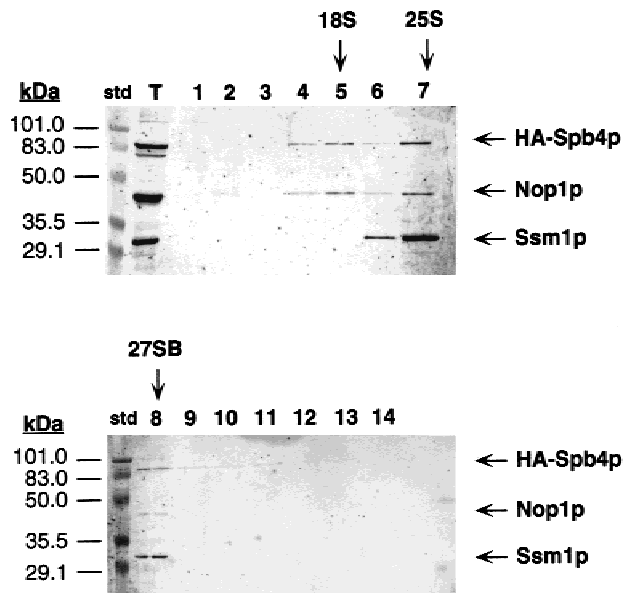
FIGURE 8. Analysis of the sedimentation of HA-Spb4p in sucrose gradients. Cells from JDY8-1A YCplac111-HA-SPB4 were grown at 30 °C and shifted to 18 °C for 12 h. Cells were harvested at an OD_{600} of 0.8. Cell extracts were resolved in 7–50% sucrose gradients containing a low concentration of Mg^{2+} to dissociate ribosomes into subunits. Fractions were collected, proteins were extracted from each fraction, and equal volumes were resolved on a 12% SDS–polyacrylamide gel and subjected to western blotting. std stands for standards for protein molecular mass determination (Bio-Rad), T for total extract and numbers correspond to fraction numbers. The same blot was decorated consecutively with different antibodies. Monoclonal mouse anti-HA 16B12, monoclonal mouse anti-Nop1p and polyclonal rabbit anti-Ssm1p antibodies were used to detect HA-Spb4p, Nop1p, and Ssm1p, respectively. Blots were decorated by the alkaline phosphatase reaction. The HA-Spb4p, Nop1p, and Ssm1p signals and the positions of the different pre-rRNAs found in the different fractions are indicated.

direct association of Spb4p with the 66S and 90S pre-ribosomal particles.

Spb4p localizes to the nucleolus

To determine whether Spb4p was also associated with the mature 60S ribosomal subunits, we identified its subcellular localization. Indirect immunofluorescence was performed with JDY8-1A YCplac111-HA-SPB4 by using anti-HA antibodies (Fig. 9B). For subnuclear localization, the nucleolus was visualized with anti-Nop1p antibodies (Fig. 9A) and the nucleoplasm was visualized by staining the DNA with DAPI (Fig. 9C). Anti-Nop1p antibodies gave the crescent-shaped staining characteristic of nucleolar proteins (Fig. 9A), which was largely excluded from the DAPI stained area (Fig. 9F). The HA-tagged Spb4p was restricted to the nucleus (Fig. 9B) and detected in the nucleolus as shown by its colocalization with Nop1p (Fig. 9D, overlap in yellow). However, in contrast to Nop1p, HA-Spb4p was also detected throughout the nucleoplasm, as shown by its colocalization with the DAPI staining (Fig 9E, overlap in

magenta). No anti-HA signal was observed using a nontagged control strain (JDY8-1A YCplac111-SPB4) (data not shown).

On the basis of these results, we conclude that Spb4 is a nuclear protein that localizes to the nucleolus and to the adjacent nucleoplasm. No cytoplasmic signal was detected, indicating that Spb4p is not associated with the mature 60S ribosomal subunits. Although the HA-Spb4 fusion protein is expressed under its own promoter from a low copy number *CEN* plasmid, some overexpression remains possible. A partial loss of function (without negative effects on growth) due to tagging might also account for the nonexclusively nucleolar localization. In any event, the presence of Spb4p in the nucleolus strongly supports a direct role for Spb4p in 60S ribosomal subunit synthesis.

DISCUSSION

In this paper, we describe the functional analysis of Spb4p. Polysome analyses and quantification of total ribosomal subunits in both a *GAL::SPB4* and the *spb4-1* strain revealed a deficit in 60S ribosomal subunits leading to the appearance of half-mer polysomes. These profiles are characteristic of mutants defective in 60S r-proteins or in *trans*-acting factors involved in its biogenesis (Kressler et al., 1998 and references therein). Detailed analyses of pre-rRNA processing by pulse-chase labeling, northern hybridization, and primer extension showed that this deficit is attributable to reduced synthesis of mature 25S and 5.8S rRNAs, as a consequence of the inhibition of pre-rRNA processing in the *GAL::SPB4* and the *spb4-1* strains.

The most striking pre-rRNA processing defect in these strains is the inhibition of the processing of the $27SB_L$ and $27SB_S$ pre-rRNAs to mature 25S and 5.8S rRNA. The 27SB pre-rRNAs are normally processed at sites C_1, at the 5′ end of the 25S rRNA, and C_2 in ITS2 (see Fig. 1). These processing reactions separate the 25S rRNA from the 7S precursor to the 5.8S rRNA and are the least well understood steps in the yeast pre-rRNA processing pathway. It is not even clear whether processing at both sites is due to endonucleolytic cleavage, or whether one site is processed by an exonuclease activity from the other. In the Spb4p-depleted strain, the 27SB pre-rRNAs show substantial accumulation as judged by northern hybridization or primer extension and are stabilized as judged by pulse-chase labeling, demonstrating that processing at sites C_1 and C_2 is inhibited. It is not clear whether Spb4p plays a direct role in processing at sites C_1 and C_2 or whether this inhibition is an indirect consequence of defects in the assembly of the pre-ribosomal particle.

In addition to these effects on the synthesis of 25S and 5.8S rRNAs, we also observed an accumulation of the 35S pre-rRNA, the appearance of an aberrant 23S product, and a reduction in the levels of the 27SA and
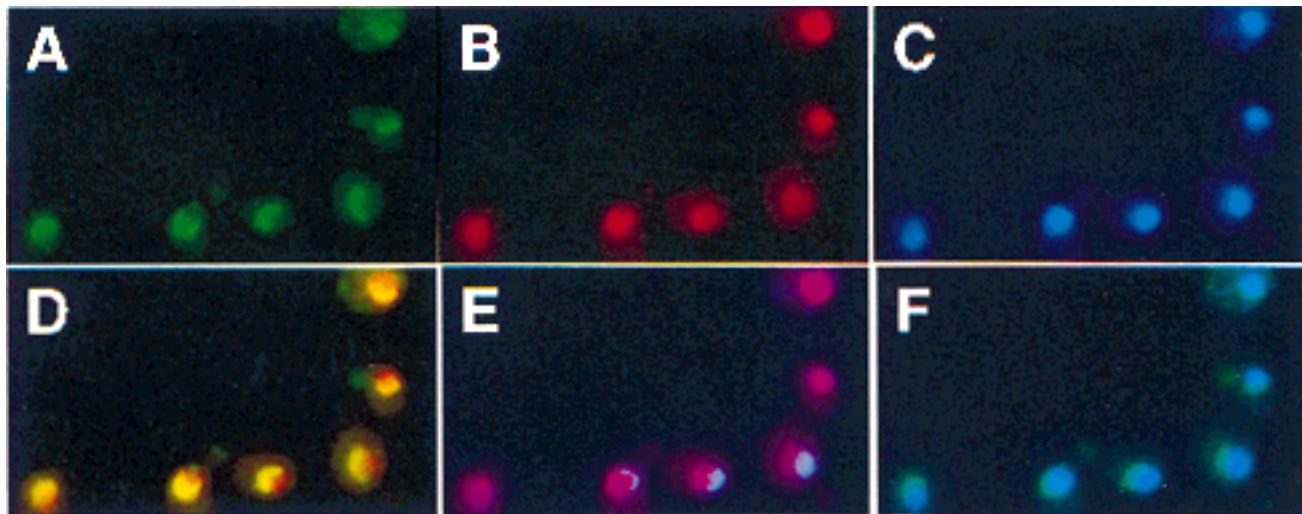
FIGURE 9. HA-Spb4p localizes to the nucleolus. Indirect immunofluorescence was performed with cells expressing HA-Spb4p from the *SPB4* promoter (JDY8-1A YCplac111-HA-SPB4). **A:** Nop1p was detected by polyclonal rabbit anti-Nop1p antibodies, followed by decoration with a goat anti-rabbit fluorescein-conjugated antibody. **B:** HA-Spb4p was detected by the monoclonal mouse anti-HA 16B12 antibody, followed by decoration with a goat anti-mouse rhodamine-conjugated antibody. **C:** Chromatin DNA was stained using 4′,6-diamidino-2-phenylindole dihydrochloride (DAPI). Pseudo-colors were assigned to the digitized micrographs (A–C) and images were merged. Overlapping distributions are revealed in: (**D**) yellow for Nop1p and HA-Spb4p colocalization; (**E**) magenta for HA-Spb4p and chromatin DNA colocalization; and (**F**) cyan for Nop1p and chromatin DNA colocalization.

20S pre-rRNAs upon depletion of Spb4p or after a shift to 18 °C of the *spb4-1* mutant. These effects are characteristic of the inhibition of pre-rRNA processing at sites A_0, A_1, and A_2 on the pathway to 18S rRNA synthesis. Similar effects have been reported previously for several other mutants affecting synthesis of the 60S ribosomal subunits. It has been proposed that this inhibition of the early processing steps is the consequence of a feedback mechanism that slows production of the 18S rRNA when the formation of 25S/5.8S rRNA is inhibited (further discussed in Zanchin et al., 1997; Daugeron & Linder, 1998; Kressler et al., 1998). This delay in 35S pre-rRNA processing seems, however, to have only a minor effect on the overall synthesis of 18S rRNA or the steady-state levels of mature 40S ribosomal subunits in the *spb4*-affected strains. The role of Spb4p in 25S/5.8S rRNA synthesis appears to be specific because neither the *spb4-1* mutation nor depletion of Spb4p significantly affects the synthesis of 5S rRNA and tRNAs or rRNA methylation.

Sucrose gradient fractionation of *spb4-1* cell extracts revealed that the accumulated 27SB pre-rRNAs are present within pre-ribosomal particles that sediment faster than the mature 60S ribosomal subunits. In wild-type cell extracts, the 27SB pre-rRNAs are found in 66S pre-ribosomes with similar sedimentation rates (Trapman et al., 1975). Sucrose gradient analysis using an HA-Spb4 fusion protein showed that almost all Spb4p in cell extracts is present in high-molecular-weight complexes. The sedimentation of these was consistent with the physical interaction of Spb4p with the 66S and 90S

pre-ribosomal particles. The population of HA-Spb4p that is not associated with the pre-ribosomal particles, as shown by its sedimentation above the 40S subunits, is clearly not the free protein. Spb4p may, therefore, be assembled with other pre-rRNA processing factors prior to its association with the pre-ribosomes. The association of Spb4p with the pre-ribosomal particles is supported by indirect immunofluorescence, which revealed that HA-Spb4p is localized to the nucleus with some nucleolar enrichment. Spb4p is not, therefore, a structural component of the 60S ribosomal subunit. The nucleoplasmic signal might represent association of Spb4p with pre-ribosomes in transit to the nuclear pores, but could also be an artifact of the expression of the HA-Spb4 fusion protein.

In many characterized mutants that are defective in synthesis of the 60S subunits, most r-proteins and the 27S pre-rRNAs are degraded rapidly. This is seen on depletion of some 60S subunit r-proteins, e.g., L16 (Moritz et al., 1990), or with mutations in *trans*-acting factors that are believed to function at early steps in the 60S ribosomal subunit assembly pathway, e.g., Nop4p/Nop77p, Dbp6p or Dbp7p (Bergès et al., 1994; Sun & Woolford, 1994; Daugeron & Linder, 1998; Kressler et al., 1998). In contrast, the accumulation of the 27SB pre-rRNAs observed in the *spb4-1* and *GAL::SPB4* strains most resembles the phenotypes described for strains depleted of Nop2p, Nop3p, or Nip7p (Russell & Tollervey, 1992; Hong et al., 1997; Zanchin et al., 1997). We speculate that Spb4p, as well as Nop2p, Nop3p, and Nip7p, are required for a late step in the 60S ribo-

somal subunit assembly. In the absence of the activity of these factors, the pre-ribosomes accumulate in a form that is relatively close to the normal structure, leading to their co-sedimentation with the normal 66S pre-ribosomes. Some structural defects, however, prevent the processing reactions at sites C_1 and C_2 from proceeding, preventing synthesis of the 25S and 5.8S rRNAs. In view of the presumed ATP-dependent RNA helicase activity of Spb4p, we assume that it normally functions in the restructuring of the pre-rRNA within the 66S pre-ribosome.

Ten putative ATP-dependent RNA helicases have been reported to function in ribosome biogenesis (see Introduction). Because most of the genes are essential for viability, we conclude that each of these proteins plays a specific, nonredundant function during ribosome biogenesis. This interpretation is supported by the fact that overexpression of other genes encoding putative RNA helicases required for the 60S ribosomal subunit synthesis (*DBP6*, *DBP7*, and *DRS1*) do not suppress either the slow-growth phenotype or the cold-sensitivity of the *spb4-1* mutant and do not bypass the lethal phenotype of the *spb4* null strain (data not shown). In addition, overexpression of *SPB4* does not suppress the slow-growth and the temperature sensitivity of *dbp6* (D. Kressler & P. Linder, unpubl.) or *dbp7* mutants (Daugeron & Linder, 1998) and double *spb4-1 dbp6* or *spb4-1 dbp7* mutants are not synthetically lethal (Daugeron & Linder, 1998 and data not shown). During the processing and modification of pre-rRNA and its assembly with the approximately 80 r-proteins, extensive structural rearrangements must occur. Furthermore, the pre-rRNAs must associate with, and dissociate from, a host of snoRNA species, some of which form very extensive base pairing with the rRNA sequences. In most cases, the rRNA–snoRNA interaction is mutually exclusive with the final folding of the rRNA in the ribosome. We therefore anticipate that more RNA helicases required for ribosome synthesis remain to be identified. In no case is the specific substrate known and determining all of their functions will be a significant challenge.

MATERIALS AND METHODS

Strains, media, and microbiological methods

The *S. cerevisiae* strains YAS168 (*MATα, spb4-1 his3 leu2 trp1 ura3*) and YAS325 (*MAT**a**/MATα, spb4::TRP1/SPB4 ade2/ade2 his3/his3 leu2/leu2 trp1/trp1 ura3/ura3*) have been described previously (Sachs & Davis, 1989, 1990). JDY8-1A (*MATα, spb4::TRP1*) is a meiotic segregant of YAS325 that requires a plasmid-borne copy of *SPB4* for cell viability. Genetic manipulations and preparation of standard media were according to established procedures (Ausubel et al., 1994; Kaiser et al., 1994). Yeast cells were transformed using a lithium acetate method (Gietz et al., 1992). *Escherichia coli*

DH10B was used for all recombinant DNA techniques (Sambrook et al., 1989).

Plasmids

Plasmid YCp50-SPB4 (*CEN-URA3*) has been described previously (Sachs & Davis, 1990). A 2.8-kb *Bam*H I–*Sal* I fragment from YCp50-SPB4 was subcloned into YCplac111 (*CEN-LEU2*) and YEplac181 (*2μm-LEU2*) (Gietz & Sugino, 1988) to generate YCplac111-SPB4 and YEplac181-SPB4, respectively. Plasmid YEplac181-DBP6 (Kressler et al., 1998) and YEplac181-DBP7 (Daugeron & Linder, 1998) have been described. The *2μm-DRS1* plasmid was a generous gift from Dr. J.L. Woolford (Carnegie Mellon University, Pittsburgh, Pennsylvania).

Construction of a *GAL::SPB4* allele and in vivo depletion of Spb4p

The *SPB4* gene was PCR amplified (Vent Polymerase, New England Biolabs) from YCplac111-SPB4 using the reverse primer (5′-AAC AGC TAT GAC CAT G-3′) and a oligonucleotide introducing the restriction site *Sal* I (5′-GCA GAA TTC GTC GAC **TCA AGT CA TTG GAA TGG GA**-3′; the *Sal* I site is underlined, and the *SPB4* ORF homology, starting with the second codon, is in bold). The PCR product was cut with *Sal* I and cloned into the *Sal* I-restricted YCplac111-based plasmid pAS24 (Schmidt et al., 1997). Correct orientation of the *Sal* I-fragment was verified by restriction analysis. The resulting construct, pAS24-SPB4, contains a *GAL1-10* promoter, a start codon followed by a double HA-tag, and the *SPB4* ORF and its 3′ contiguous region. This plasmid was transformed into the strain JDY8-1A YCp50-SPB4. The subsequent counter-selection of the *URA3 SPB4* harboring plasmid on 5-FOA plates containing galactose resulted in the strain JDY8-1A pAS24-SPB4. The plasmid pAS24-SPB4 complemented the *spb4* null strain to the wild-type extent on medium containing galactose (YPGal) at all the tested temperatures (18, 30, and 37 °C). We also refer to this strain as the *GAL::SPB4* strain or, if grown in medium containing glucose (YPD), as the Spb4p-depleted strain.

For in vivo depletion of Spb4p, JDY8-1A pAS24-SPB4 was grown in liquid YPGal until mid-exponential phase. Cells were harvested, washed, and used to inoculate YPD cultures. Cell growth was monitored over a period of 36 h, during which the cultures were regularly diluted into fresh YPD medium to maintain exponential growth. As a control, JDY8-1A YCplac111-SPB4 was used. Samples for western blot analyses, polysome analyses, and RNA extraction were taken at different times.

Sucrose gradient analyses

Polyribosome preparations, polysome analyses, and ribosomal subunit preparations were done according to Foiani et al. (1991), exactly as described (Kressler et al., 1997). Gradient analysis was performed using an ISCO UV-6 gradient collector and monitored continuously at A_{254}.

For fractionation analyses, low Mg^{2+} gradients identical to those used for ribosomal subunit quantification were pre-

pared. After centrifugation, fractions of 0.5 mL were collected manually. For RNA analysis, 0.4 mL of each fraction was adjusted to a final concentration of 10 mM Tris-HCl, pH 7.5, 10 mM EDTA, and 0.5% SDS. Total RNA was isolated by two consecutive extractions with 10 mM Tris-HCl, pH 7.5, saturated phenol:chloroform:isoamyl alcohol (25:24:1), followed by a chloroform:isoamyl alcohol (24:1) extraction. Then, RNA was precipitated with ethanol in the presence of 0.3 M sodium acetate, pH 5.2. Finally, RNA pellets were dissolved in 20 μL of distilled water and 5 μL was resolved on 1.2% agarose–6% formaldehyde gels as described (Venema et al., 1998). For western analysis, proteins (0.1 mL of each fraction) were precipitated by addition of trichloroacetic acid to a final concentration of 10%, followed by incubation on ice for at least 10 min. Proteins were pelleted by centrifugation in a microfuge for 10 min at 4 °C. Pellets were washed twice with 1 mL ice-cold acetone and finally resuspended in 20 μL of protein gel loading buffer (Ausubel et al., 1994). Aliquots of 10 μL were loaded onto SDS-polyacrylamide gels and analyzed by western blot analysis according to standard procedures (Sambrook et al., 1989; Ausubel et al., 1994). Monoclonal mouse anti-HA 16B12 (BabCo), monoclonal mouse anti-Nop1p (Aris & Blobel, 1988), and polyclonal rabbit anti-Ssm1p (Petitjean et al., 1995) antibodies were used as primary antibodies. Blots were decorated with alkaline phosphatase conjugated secondary antibodies (Bio-Rad).

SPB4 HA epitope tagging and cloning under the control of its cognate promoter

To express an N-terminally HA-tagged Spb4 fusion protein from its cognate promoter at approximately wild-type levels, the *SPB4* promoter was PCR amplified from YCplac111-SPB4 with the universal primer (5′-GTA AAA CGA CGG CCA GT-3′) and an oligonucleotide introducing an *Xba* I site (5′-CGC TAG <u>TCT AGA</u> TGC **CAT TGT TTT TAT TGC TGC TG**-3′; the *Xba* I site is underlined, the reverse complement of the start codon is in bold and underlined, and the reverse complement of the *SPB4* promoter sequence is in bold). The PCR product was digested with *Eco*R I and *Xba* I, and cloned together with the *Xba* I/*Bam*H I-released HA tag of plasmid pAS24 into the *Eco*R I/*Bam*H I-restricted plasmid pAS24-SPB4. Then, the 1.6-kb *Sph* I fragment from the above plasmid was replaced by the same fragment from YCplac111-SPB4. The *SPB4* ORF sequences still originating from the PCR were verified by sequencing. The resulting plasmid, YCplac111-HA-SPB4, complemented the *spb4* null allele to the wild-type extent at all the tested temperatures (18, 30, and 37 °C) and the HA-tagged Spb4p was detected by western blotting as a band that migrated at the molecular mass of approximately 85 kDa.

Indirect immunofluorescence

The strains JDY8-1A YCplac111-HA-SPB4 and JDY8-1A YCplac111-SPB4 were grown up to an OD_{600} of around 0.5 in YPD medium and 2.5 OD_{600} units were harvested by centrifugation. Preparations of yeast cells for immunofluorescence were done according to standard procedures (Pringle et al., 1991). DAPI (4′,6-diamidino-2-phenylindole dihydrochloride, Fluka) was used to stain DNA. Primary monoclonal mouse

anti-HA antibodies 16B12, at a dilution of 1:200, and secondary goat anti-mouse rhodamine conjugated antibodies (Pierce), at a dilution of 1:200, were used to detect HA-Spb4p. Polyclonal rabbit anti-Nop1p antibodies at a dilution of 1:500, and secondary goat anti-rabbit fluorescein conjugated antibodies (Pierce), at a dilution of 1:200, were used to detect the nucleolar protein Nop1p (Tollervey et al., 1991). Fluorescently labeled cells were inspected in a Zeiss Axiophot fluorescence microscope using the Plan-NEOFLUAR 100×/1.3 objective, and images were acquired with a cooled CCD camera (Princeton Instruments) controlled by a Power Macintosh 8500/100 computer. Images were adjusted to similar output intensities, pseudo-colors were assigned and images were merged using Adobe Photoshop 3.0. Figures were printed on a Kodak Digital Science 8650 PS Color Printer.

RNA analyses

Pulse-chase labeling of pre-rRNA was performed as described previously (Kressler et al., 1998), using 250 μCi [*methyl*-^{3}H]methionine (Amersham, 70–85 Ci/mmol) or 100 μCi [5,6-^{3}H]uracil (Amersham, 45–50 Ci/mmol) per 40 OD_{600} of yeast cells. Total RNA was extracted by the acid-phenol method (Ausubel et al., 1994).

Steady-state levels of pre-rRNAs were assessed by northern and primer extension analyses according to Venema et al. (1998). Total RNA was extracted as above from aliquots of 10 OD_{600} of exponentially growing cells. Oligonucleotides 5′A_0, 18S, D/A_2, A_2/A_3, A_3/B_1, 5.8S, E/C_2, C_1/C_2, 25S (as numbered from 1 to 9 according to Fig. 1A), and 5S have been described previously (de la Cruz et al., 1998). Prior to northern hybridization or primer extension analysis, they were end labeled with 30 μCi [γ-^{32}P]ATP (Amersham, 5,000 Ci/mmol) using T4 Polynucleotide kinase (Appligene).

ACKNOWLEDGMENTS

Manuscript accepted without revision July 13, 1998

REFERENCES

Aris JP, Blobel G. 1988. Identification and characterization of a yeast nucleolar protein that is similar to a rat liver nucleolar protein. *J Cell Biol 107*:17–31.

Ausubel FM, Brent R, Kingston RE, Moore DD, Seidman JG, Smith JA, Struhl K. 1994. *Saccharomyces cerevisiae*. In: *Current protocols in molecular biology*. New York: John Wiley & Sons, Inc. pp 13.0.1–13.14.17.

Bergès T, Petfalski E, Tollervey D, Hurt EC. 1994. Synthetic lethality with fibrillarin identifies NOP77p, a nucleolar protein required for pre-rRNA processing and modification. *EMBO J 13*:3136–3148.

Czaplinski K, Weng Y, Hagan KW, Peltz SW. 1995. Purification and characterization of the Upf1 protein: A factor involved in translation and mRNA degradation. *RNA 1*:610–623.

Daugeron MC, Linder P. 1998. Dbp7p, a putative ATP-dependent RNA helicase from *Saccharomyces cerevisiae*, is required for 60S ribosomal subunit assembly. *RNA 4*:566–581.

de la Cruz J, Kressler D, Tollervey D, Linder P. 1998. Dob1p (Mtr4p) is a putative ATP-dependent RNA helicase required for the 3′ end formation of 5.8S rRNA in *Saccharomyces cerevisiae*. *EMBO J 17*:1128–1140.

Eichler DC, Craig N. 1994. Processing of eukaryotic ribosomal RNA. *Prog Nucleic Acid Res Mol Biol 49*:197–239.

Foiani M, Cigan AM, Paddon CJ, Harashima S, Hinnebusch AG. 1991. GCD2, a translational repressor of the *GCN4* gene, has a general function in the initiation of protein synthesis in *Saccharomyces cerevisiae*. *Mol Cell Biol 11*:3203–3216.

Fuller-Pace FV. 1994. RNA helicases: Modulators of RNA structure. *Trends Cell Biol 4*:271–274.

Gietz D, St. Jean A, Woods RA, Schiestl RH. 1992. Improved method for high efficiency transformation of intact yeast cells. *Nucleic Acids Res 20*:1425.

Gietz RD, Sugino A. 1988. New yeast–*Escherichia coli* shuttle vectors constructed with in vitro mutagenized yeast genes lacking six-base pair restriction sites. *Gene 74*:527–534.

Hong B, Brockenbrough JS, Wu P, Aris JP. 1997. Nop2p is required for pre-rRNA processing and 60S ribosome subunit synthesis in yeast. *Mol Cell Biol 17*:378–388.

Jacobs Anderson JS, Parker R. 1996. RNA turnover: The helicase story unwinds. *Curr Biol 6*:780–782.

Kaiser C, Michaelis S, Mitchell A. 1994. *Methods in yeast genetics: A Cold Spring Harbor Laboratory course manual*. Cold Spring Harbor, New York: Cold Spring Harbor Laboratory Press.

Kim SH, Smith J, Claude A, Lin RJ. 1992. The purified yeast pre-mRNA splicing factor PRP2 is an RNA-dependent NTPase. *EMBO J 11*:2319–2326.

Kressler D, de la Cruz J, Rojo M, Linder P. 1997. Fal1p is an essential DEAD-box protein involved in 40S-ribosomal-subunit biogenesis in *Saccharomyces cerevisiae*. *Mol Cell Biol 17*:7283–7294.

Kressler D, de la Cruz J, Rojo M, Linder P. 1998. Dbp6p is an essential putative ATP-dependent RNA helicase required for 60S-ribosomal-subunit assembly in *Saccharomyces cerevisiae*. *Mol Cell Biol 18*:1855–1865.

Kruiswijk T, Planta RJ, Krop JM. 1978. The course of the assembly of ribosomal subunits in yeast. *Biochim Biophys Acta 517*:378–389.

Liang WQ, Clark JA, Fournier MJ. 1997. The rRNA-processing function of the yeast U14 small nucleolar RNA can be rescued by a conserved RNA helicase-like protein. *Mol Cell Biol 17*:4124–4132.

Mélèse T, Xue Z. 1995. The nucleolus: An organelle formed by the act of building a ribosome. *Curr Opin Cell Biol 7*:319–324.

Moritz M, Paulovich AG, Tsay YF, Woolford JL Jr. 1990. Depletion of yeast ribosomal proteins L16 and rp59 disrupt ribosomal assembly. *J Cell Biol 111*:2261–2274.

O'Day CL, Chavanikamannil F, Abelson J. 1996a. 18S rRNA processing requires the RNA helicase-like protein Rrp3. *Nucleic Acids Res 24*:3201–3207.

O'Day CL, Dalbadie-McFarland G, Abelson J. 1996b. The *Saccharomyces cerevisiae* Prp5 protein has RNA-dependent ATPase activity with specificity for U2 small nuclear RNA. *J Biol Chem 271*:33261–33267.

Petitjean A, Bonneaud N, Lacroute F. 1995. The duplicated *Saccharomyces cerevisiae* gene *SSM1* encodes a eucaryotic homolog of the eubacterial and archeabacterial L1 ribosomal proteins. *Mol Cell Biol 15*:5071–5081.

Pringle JR, Adams AEM, Drubin DG, Haarer BK. 1991. Immunofluorescence methods for yeast. *Methods Enzymol 194*:565–602.

Ripmaster TL, Vaughn GP, Woolford JL Jr. 1992. A putative ATP-dependent RNA helicase involved in *Saccharomyces cerevisiae* ribosome assembly. *Proc Natl Acad Sci USA 89*:11131–11135.

Rozen F, Edery I, Meerovitch K, Dever TE, Merrick WC, Sonenberg N. 1990. Bidirectional RNA helicase activity of eucaryotic translation initiation factors 4A and 4F. *Mol Cell Biol 10*:1134–1144.

Russell ID, Tollervey D. 1992. NOP3 is an essential yeast protein which is required for pre-rRNA processing. *J Cell Biol 119*:737–747.

Sachs AB, Davis RW. 1989. The poly(A) binding protein is required for poly(A) shortening and 60S ribosomal subunit-dependent translation initiation. *Cell 58*:857–867.

Sachs AB, Davis RW. 1990. Translation initiation and ribosomal biogenesis: Involvement of a putative rRNA helicase and *RPL46*. *Science 247*:1077–1079.

Sambrook J, Fritsch EF, Maniatis T. 1989. *Molecular cloning: A laboratory manual*. Cold Spring Harbor, New York: Cold Spring Harbor Laboratory Press.

Schmid SR, Linder P. 1992. D-E-A-D protein family of putative RNA helicases. *Mol Microbiol 6*:283–292.

Schmidt A, Bickle M, Beck T, Hall MN. 1997. The yeast phosphatidylinositol kinase homolog TOR2 activates RHO1 and RHO2 via the exchange factor ROM2. *Cell 88*:531–542.

Schwer B, Gross CH. 1998. Prp22, a DExH-box RNA helicase, plays two distinct roles in yeast pre-mRNA splicing. *EMBO J 17*:2986–2094.

Snay-Hodge CA, Colot HV, Goldstein AL, Cole CN. 1998. Dbp5p/Rat8p is a yeast nuclear pore-associated DEAD-box protein essential for RNA export. *EMBO J 17*:2663–2676.

Staley JP, Guthrie C. 1998. Mechanical devices of the spliceosome: Motors, clocks, springs, and things. *Cell 92*:315–326.

Sun C, Woolford JL Jr. 1994. The yeast *NOP4* gene product is an essential nucleolar protein required for pre-rRNA processing and accumulation of 60S ribosomal subunits. *EMBO J 13*:3127–3135.

Tollervey D, Kiss T. 1997. Function and synthesis of small nucleolar RNAs. *Curr Opin Cell Biol 9*:337–342.

Tollervey D, Lehtonen H, Carmo-Fonseca M, Hurt EC. 1991. The small nucleolar RNP protein NOP1 (fibrillarin) is required for pre-rRNA processing in yeast. *EMBO J 10*:573–583.

Trapman J, Planta RJ. 1976. Maturation of ribosomes in yeast. I. Kinetic analysis by labelling of high molecular weight rRNA species. *Biochim Biophys Acta 442*:265–274.

Trapman J, Retèl J, Planta RJ. 1975. Ribosomal precursor particles from yeast. *Exp Cell Res 90*:95–104.

Tseng SSI, Weaver PL, Liu Y, Hitomi M, Tartakoff AM, Chang TH. 1998. Dbp5p, a cytosolic RNA helicase, is required for poly(A)+ RNA export. *EMBO J 17*:2651–2662.

Udem SA, Warner JR. 1973. The cytoplasmic maturation of a ribosomal precursor ribonucleic acid in yeast. *J Biol Chem 248*:1412–1416.

van Nues RW, Venema J, Rientjes JMJ, Dirks-Mulder A, Raué HA. 1995. Processing of eukaryotic pre-rRNA: The role of the transcribed spacers. *Biochem Cell Biol 73*:789–801.

Venema J, Bousquet-Antonelli C, Gelugne JP, Caizergues-Ferrer M, Tollervey D. 1997. Rok1p is a putative RNA helicase required for rRNA processing. *Mol Cell Biol 17*:3398–3407.

Venema J, Planta RJ, Raué HA. 1998. In vivo mutational analysis of ribosomal RNA in *Saccharomyces cerevisiae*. In: Martin R, ed. *Protein synthesis: Methods and protocols*. Totowa, New Jersey: Humana Press. Forthcoming.

Venema J, Tollervey D. 1995. Processing of pre-ribosomal RNA in *Saccharomyces cerevisiae*. *Yeast 11*:1629–1650.

Wang Y, Wagner JDO, Guthrie C. 1998. The DEAH-box slicing factor Prp16 unwinds RNA duplexes in vitro. *Curr Biol 8*:441–461.

Weaver PL, Sun C, Chang TH. 1997. Dbp3p, a putative RNA helicase in *Saccharomyces cerevisiae*, is required for efficient pre-rRNA processing predominantly at site A_3. *Mol Cell Biol 17*:1354–1365.

Woolford JL Jr, Warner JR. 1991. The ribosome and its synthesis. In: Broach JR, Pringle JR, Jones EW, eds. *The molecular and cellular biology of the yeast Saccharomyces. Genome dynamics, protein synthesis, and energetics*. Cold Spring Harbor, New York: Cold Spring Harbor Laboratory Press. pp 587–626.

Zanchin NIT, Roberts P, de Silva A, Sherman F, Goldfarb DS. 1997. *Saccharomyces cerevisiae* Nip7p is required for efficient 60S ribosome subunit biogenesis. *Mol Cell Biol 17*:5001–5015.